Journal of Marine Science and Technology

Volume 28 | Issue 2 Article 5

USING THE CHLORIDE PENETRATION DEPTH OBTAINED FROM RCPT TO ASSESS THE PERMEABILITY OF CONCRETE

Kang-Shiun Huang
Department of Harbor and River Engineering, National Taiwan Ocean University, 2 Pei-Ning Road, Keelung, Taiwan

Chung-Chia Yang
Department of Harbor and River Engineering, National Taiwan Ocean University, 2 Pei-Ning Road, Keelung, Taiwan, ccyang@mail.ntou.edu.tw

Recommended Citation

Huang, Kang-Shiun and Yang, Chung-Chia (2020) "USING THE CHLORIDE PENETRATION DEPTH OBTAINED FROM RCPT TO ASSESS THE PERMEABILITY OF CONCRETE," *Journal of Marine Science and Technology*: Vol. 28: Iss. 2, Article 5.
DOI: 10.6119/JMST.202004_28(2).0005
Available at: https://jmstt.ntou.edu.tw/journal/vol28/iss2/5

USING THE CHLORIDE PENETRATION DEPTH OBTAINED FROM RCPT TO ASSESS THE PERMEABILITY OF CONCRETE

Acknowledgements

The financial support of Ministry of Science and Technology, ROC, under the grants MOST 108-2221-E-019- 008-MY2 is gratefully appreciated.

Journal of Marine Science and Technology, Vol. 28, No. 2, pp. 120-130 (2020)
DOI: 10.6119/JMST.202004_28(2).0005

USING THE CHLORIDE PENETRATION DEPTH OBTAINED FROM RCPT TO ASSESS THE PERMEABILITY OF CONCRETE

Kang-Shiun Huang and Chung-Chia Yang

Key words: RCPT, durability, electrical properties, fly ash.

ABSTRACT

A review of the literature on the rapid chloride permeability test (RCPT; ASTM C1202) indicates that RCPT has a few shortcomings, namely complex anions in concrete and Joule heating. The charge passed through concrete is affected by chloride ions because of the complex anions in concrete. Moreover, Joule heating influences the experimental temperature and causes an abnormal increase in the charge passed. Engineers have focused on the advance of the critical chloride front toward steel, but the charge passed in RCPT experiments has a poor relationship with the chloride penetration depth in fly ash concrete. Thus, it is risky to use RCPT to assess the durability of fly ash concrete. In this study, we subjected ordinary Portland cement concrete and fly ash concrete to RCPT. After RCPT, the chloride profiles of the specimens were determined using a modified version of RCPT. Based on the linear relationship found between the charge passed during RCPT and the total amount of chloride obtained from the chloride profile, the chloride profile can be obtained by measuring the charge passed and the surface chloride content. In addition, the chloride penetration depth obtained from the chloride profile was used to assess the chloride permeability of concrete.

I. INTRODUCTION

The rapid chloride permeability test (RCPT), designated ASTM C1202, is used for rapid qualitative assessment of the chloride permeability of concrete. The RCPT standard specifies the chloride permeability rating of concrete based on the charge passed through a specimen over a 6-h test. In recent years, RCPT has been mainly used to assess the resistance of concrete to the penetration of chloride ions. In addition, RCPT has been used to investigate (1) the effects of mineral admixtures on the resistance of concrete to chloride ion penetration (Bagheri et al. 2012, Bernal et al. 2012, Ramezanianpour and Jovein 2012, Morozov et al. 2013, Ravikumar and Neithalath 2013), (2) surface treatments (Yoon et al. 2012, Yang et al. 2004), (3) aggregate fraction (Wee et al. 1999, Yang and Su 2002), (4) curing condition (Aldea et al. 2000), and (5) cracking of concrete (Lim et al. 2000, Park et al. 2012) due to the penetration of chloride ions.

Based on a review of the literature on RCPT, Feldman et al. (1999) derived a favorable correlation between the total charge passed and both the initial current and the electrical conductivity measured at the start of a test. McCarter et al. (2000) reported that the conductivity of the free pore fluid increases as the temperature increases and that the applied electrical potential for RCPT heats the concrete specimen, thus affecting the flow speed. Julio-Betancourt and Hooton (2004) suggested that the application of a linear correlation between the total charge and temperature (in addition to using RCPT equipment to perform a 1-min conductivity test) could be a practical measure for improving the RCPT standard. Pfeifer et al. (1994) mentioned that reliable correlations might not exist between the results of RCPT and a 90-day salt ponding test. McGrath and Hooton (1999) found a poor correlation between the RCPT results obtained after passing a charge for 6 h and the integral chloride content obtained from a 90-day salt ponding test. The integral chloride content did not accurately represent the chloride penetration depth. Shi (2004) observed that ion transportation in concrete depends on the pore structure of the concrete, whereas RCPT results depend on both the pore structure characteristics and the electrical conductivity of the pore solution. Thus, it is inappropriate to use RCPT results to rank the chloride permeability of concrete when blast furnace slag, fly ash, and silica fumes are used in concrete.

The most direct approach to overcoming these shortcomings involves measuring the chloride penetration depth of a specimen after RCPT. Tang and Nilsson (1992) first used the concept of chloride penetration depth in electrochemical experiments on cementitious materials. However, the traditional method involved three laborious experimental procedures, namely milling the specimen layer by layer, extracting the

Paper submitted 12/23/19; revised 01/02/20; accepted 03/03/20. Author for correspondence: Chung-Chia Yang (E-Mail: ccyang@mail.ntou.edu.tw).
Department of Harbor and River Engineering, National Taiwan Ocean University, 2 Pei-Ning Road, Keelung, Taiwan

Table 1. Mixture proportions.

Mix	w/b	Unit content: kg/m^3					
		Water	Cement	Fly ash	Coarse aggregate	Fine aggregate	SP
F0-30	0.3	160	533	0	956	790	5.3
F0-35	0.35	160	457	0	956	856	4.6
F0-40	0.4	160	400	0	956	915	0
F0-45	0.45	160	356	0	956	953	0
F0-50	0.5	160	320	0	956	983	0
F0-55	0.55	160	291	0	956	1008	0
F0-60	0.6	160	267	0	956	1028	0
F0-65	0.65	160	246	0	956	1046	0
F20-35	0.35	160	366	91	956	825	4.6
F20-45	0.45	160	284	71	956	928	0
F20-55	0.55	160	233	58	956	987	0
F20-65	0.65	160	197	49	956	1028	0
F30-35	0.35	160	320	137	956	809	4.6
F30-45	0.45	160	249	107	956	908	0
F30-55	0.55	160	204	87	956	971	0
F30-65	0.65	160	172	74	956	1015	0
F40-35	0.35	160	274	183	956	793	4.6
F40-45	0.45	160	213	142	956	896	0
F40-55	0.55	160	175	116	956	961	0
F40-65	0.65	160	148	98	956	1006	0
F50-35	0.35	160	229	229	956	777	4.6
F50-45	0.45	160	178	178	956	891	0
F50-55	0.55	160	145	145	956	957	0
F50-65	0.65	160	123	123	956	1003	0

chloride content at each sample depth, and determining the chloride profile. To reduce this tedium, Tang (1996) combined the results of two studies (Otsuki et al. 1992; Nagataki et al. 1993) to develop the colorimetric method. The colorimetric method, which involves spraying 0.1M silver nitrate solution and measuring white silver chloride, greatly simplified the process of determining the chloride penetration depth. However, a few studies (Andrade et al. 1999; Meak and Sirvivatnanon, 2003) have found that the chloride concentration at the color change boundary of silver nitrate is not constant, and chloride penetration depths have a higher coefficient of variation in the colorimetric method. Thus, use of the colorimetric method to evaluate the durability of concrete introduces experimental bias.

In this study, we used two types of concrete, namely ordinary Portland cement (OPC) concrete and fly ash concrete, to conduct RCPT and obtain the traditional chloride profiles of specimens after the completion of RCPT. Furthermore, the modified RCPT was employed to reduce the tedium of the traditional method and overcome the inaccuracies of the colorimetric method. The relationship between the charge passed and the total amount of chloride was used to reduce the experimental procedures of the traditional method. Then, the modified chloride profile was applied to eliminate the experimental bias associated with the colorimetric method. Finally, the modified RCPT method based on the chloride penetration depth was used to assess the chloride permeability of OPC concrete and fly ash concrete.

II. EXPERIMENTAL PROGRAM

1. Materials and specimens

ASTM Type I Portland cement and F-type fly ash were used as binders. River sand was used as the fine aggregate, and crushed limestone with a maximum size of 10 mm was used as the coarse aggregate. Table 1 lists the proportions of various materials used in the concrete. Five series binders (F0, F20, F30, F40, and F50), each with different w/b ratios, were used. Series F0 represents OPC concrete, and 20%, 30%, 40%, and 50% of the cement used in series F0 was replaced with fly ash in the series F20, F30, F40, and F50 concretes, respectively. For each mix, numerous cylindrical specimens (ϕ 100 × 200 mm) were cast and cured. After demolding, the specimens were cured in water (23°C) for 56 days. For RCPT, specimens with a thickness of 50 mm and diameter of 100 mm were cut from the central portion of the cast cylinders. To prevent heterogeneity, the specimens were vacuum-saturated before testing, as described in ASTM C1202.

Table 2. The 6 h charge passed from RCPT.

Mix	Charge passed (coulomb)			
	Specimen 1	Specimen 2	Specimen 3	Average
F0-30	1880	1881	1921	1894
F0-35	2190	2195	2215	2200
F0-40	2381	2391	2413	2395
F0-45	3023	3042	3142	3069
F0-50	3785	3792	3819	3799
F0-55	4234	4246	4381	4287
F0-60	4864	4985	4932	4927
F0-65	5481	5486	5572	5513
F20-35	981	971	997	983
F20-45	1300	1335	1271	1302
F20-55	1657	1622	1685	1655
F20-65	1994	2042	1958	1998
F30-35	453	455	467	458
F30-45	871	870	890	877
F30-55	1092	1094	1119	1102
F30-65	1303	1330	1381	1338
F40-35	361	366	392	373
F40-45	502	511	563	525
F40-55	701	712	765	726
F40-65	1051	1066	1108	1075
F50-35	305	306	362	324
F50-45	433	441	471	448
F50-55	1003	1013	1063	1026
F50-65	1227	1231	1274	1244

2. RCPT and chloride profile determined after RCPT

In RCPT, a vacuum-saturated, 50-mm-thick specimen was placed between two acrylic cells. One of the cells was filled with a 0.30-mole/L NaOH solution and the other was filled with a 0.52-mole/L NaCl solution. The cells were connected to a 60-V power source. Current was measured and recorded using a data logger, and the total charge passed through the specimen was computed by integrating the current and time. After RCPT, the solutions in the cells were removed, and the specimens were allowed to dry. Thereafter, the surface of each specimen was wire-brushed until all salt crystal buildup was completely removed. A profile grinder (PF-1100) was used for grinding and collecting powder samples of concrete from a specified depth relative to the specimen surface. The chloride ion content at every incremental depth was determined using the powders ground in accordance with AASHTO T260.

III. RESULTS AND DISCUSSION

1. Charge passed obtained using RCPT

RCPT was used to determine the permeability of various types of concrete to chloride ions within a relatively short period. In RCPT, the current passed through the concrete specimens in the first 6 h was measured, and the resistance of the concrete to chloride ion penetration was assessed based on the total charge passed within 6 h. The total charge passed Q was determined by integrating the current-time curve as follows:

$$Q = \int I(t)\, dt, \tag{1}$$

where

$I(t)$: time-dependent total electrical current,

t: elapsed time.

Table 2 lists the values of Q obtained using the RCPT for all mixes. A replacement of 20% (F20) and 30% (F30) of cement with fly ash decreases the charge passed to approximately 55% to 64% and 71% to 79% that of Portland cement concrete (F0), respectively. When the replacement increases to 40% and 50%, it decreases the charge value to approximately 80% to 83% and 76% to 85% that of Portland cement concrete, respectively. The use of fly ash can significantly reduce the charge passed during the RCPT.

2. Chloride profile obtained after RCPT

After the completion of RCPT, Specimen 1 (Table 2) was

Table 3. Main results of the chloride profile.

Mix	C_s (%)	a	R^2	m (%)	d (cm)
F0-30	0.305	1.149	0.995	0.252	1.72
F0-35	0.297	0.794	0.989	0.295	2.07
F0-40	0.266	0.555	0.985	0.316	2.43
F0-45	0.261	0.333	0.992	0.401	3.13
F0-50	0.220	0.154	0.996	0.496	4.48
F0-55	0.136	0.009	0.137	1.300	-
F0-60	0.144	0.018	0.659	0.939	-
F0-65	0.132	0.011	0.316	1.126	-
F20-35	0.182	3.581	0.989	0.085	0.90
F20-45	0.173	1.050	0.997	0.150	1.65
F20-55	0.169	0.656	0.990	0.185	2.08
F20-65	0.150	0.370	0.994	0.218	2.70
F30-35	0.170	6.790	0.977	0.058	0.65
F30-45	0.166	2.188	0.987	0.099	1.13
F30-55	0.155	1.114	0.988	0.130	1.57
F30-65	0.143	0.577	0.995	0.167	2.15
F40-35	0.143	6.315	0.976	0.050	0.65
F40-45	0.133	2.058	0.951	0.082	1.12
F40-55	0.125	1.092	0.982	0.106	1.52
F40-65	0.124	0.631	0.948	0.138	2.00
F50-35	0.106	4.111	0.963	0.046	0.76
F50-45	0.097	1.296	0.963	0.076	1.32
F50-55	0.150	0.655	0.981	0.164	2.03
F50-65	0.169	0.582	0.988	0.196	2.20

examined for all mixes by collecting concrete powder samples from different depths post the completion of chloride migration.

2.1. Chloride profile

To obtain the chloride profile curve, the experimental data were fitted using nonlinear regression analysis:

$$C = C_s \cdot \exp\left(-ax^2\right), \tag{2}$$

where

C: chloride content, (%, wt. specimen).

C_s: surface chloride content, $x = 0$, (%, wt. specimen).

a: experimental constant.

Eq. (2) was fitted using a commercial curve-fitting software program to search for a nonlinear, least-square, best fit for the experimental data. The least-square regression searches for the highest coefficient of determination (R^2). Table 3 lists the surface chloride content (C_s), correlation coefficient (R^2), and experimental constant (a) for all test specimens. The experimental results and chloride profiles of series F0 and F20 concrete are shown in Figs. 1 and 2, respectively. Fig. 1(b) shows that the chloride ions passed through the specimen and reached the anode cell. As shown in Fig. 1(a), the surface chloride content (C_s) decreased as the w/b ratio increased for the series F0 concrete specimen. The surface chloride contents listed in Table 3 and shown in Figs. 1 and 2 indicate that the use of fly ash can reduce the surface chloride content at the end of RCPT.

2.2. Chloride penetration depth

The chloride penetration depth is calculated from the chloride profile, and in this study, a value of 0.01% chloride was applied, as shown in Fig. 3. Based on Eq. (2), the chloride penetration depth (d) was calculated as follows:

$$d = \left(\frac{-\ln\left(0.01/C_s\right)}{a}\right)^{0.5}. \tag{3}$$

Eq. (3) yields the chloride penetration depths obtained from the chloride profiles of all mixes, as listed in Table 3.

Figure 4 illustrates the relationship between the charge passed and the chloride penetration depths for all mixes except F0-60 and F0-65. The results obtained by testing concrete with fly ash and OPC were subjected to linear regression analysis separately. The empirical relationship between the charge passed and the chloride penetration depth for OPC concrete was statistically derived using the following equation:

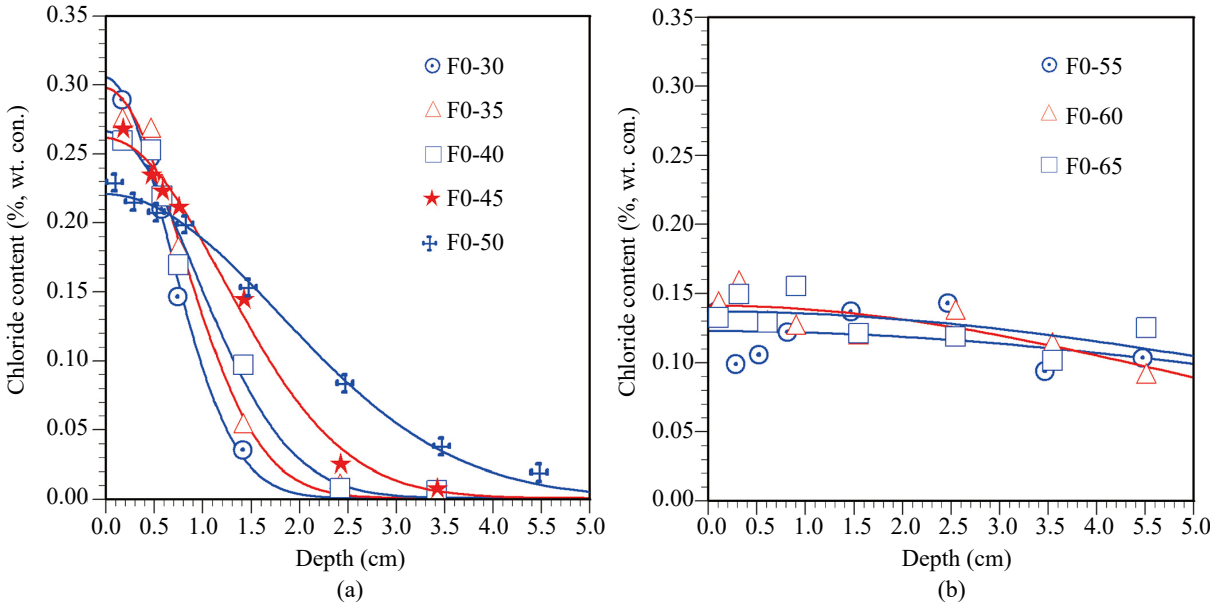

Fig. 1. The experimental result and the chloride profiles: (a) F0-30 to F0-50, (b) F0-55 to F0-60.

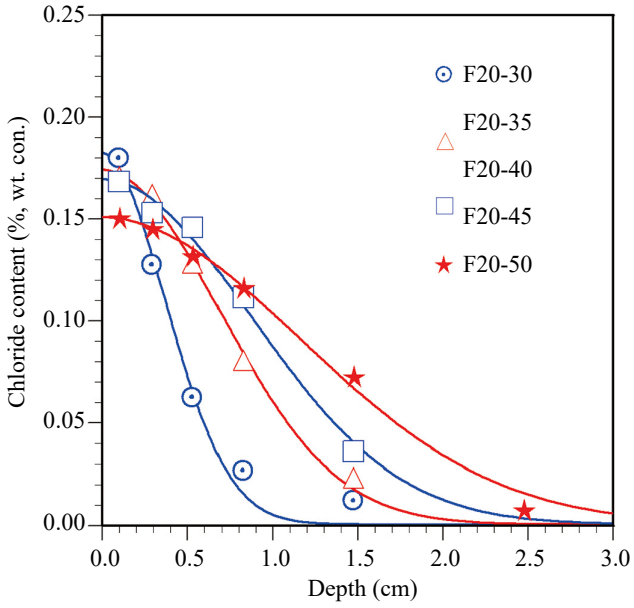

Fig. 2. The experimental result and the chloride profiles for series F20.

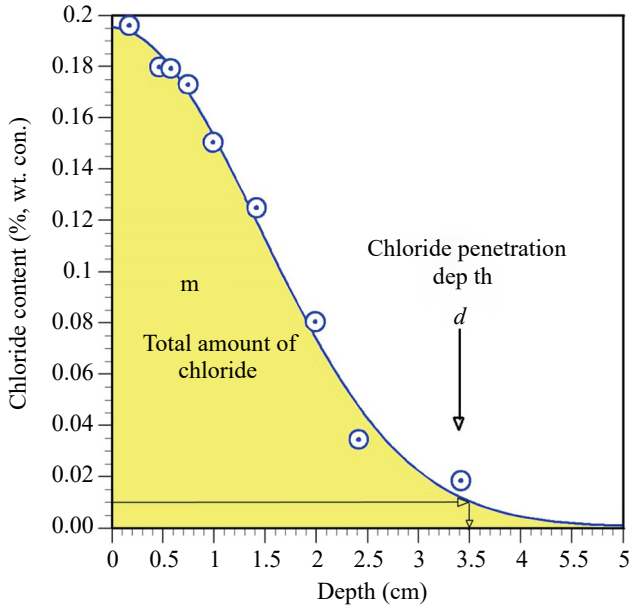

Fig. 3. Typical chloride profile obtained after RCPT.

$$d = 1.42 \times 10^{-3} Q - 1.02, \quad (4)$$

where

d: chloride penetration depth in cm,

Q: charge passed in Coulomb.

The correlation coefficient R^2 was 0.99, which indicated a strong linear correlation between d and Q for OPC concrete. The above results (Eq. (4)) indicate that it is appropriate to use the charge passed through the specimen to estimate the chloride penetration depth for OPC concrete because of the strong linear relationship between d and Q. Eq. (4) was used to determine the chloride penetration depths corresponding to the charges passed of 1000 C, 2000 C, and 4000 C. The chloride permeability ratings of concrete listed in Table 4 were computed based on the penetration depth and the charge passed through the specimen during the 6-h test.

The empirical relationship between the charge passed and the chloride penetration depth for fly ash concrete was statistically derived by forcing a linear regression analysis through zero:

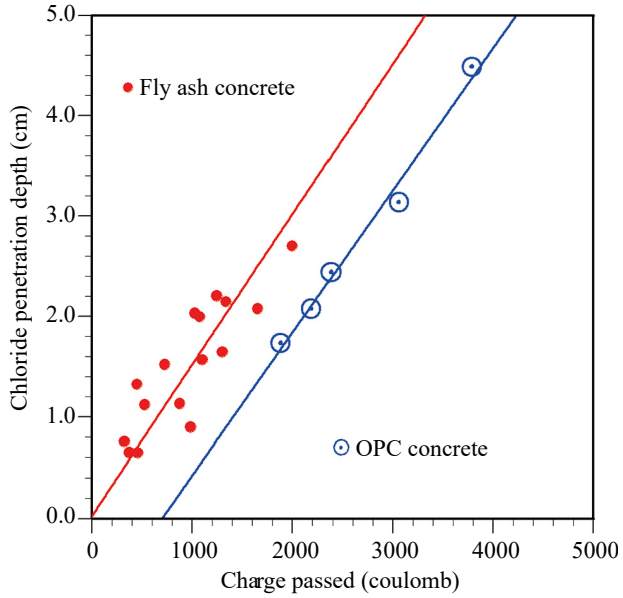

Fig. 4. The relationship between the charge passed and the penetration depth of chloride.

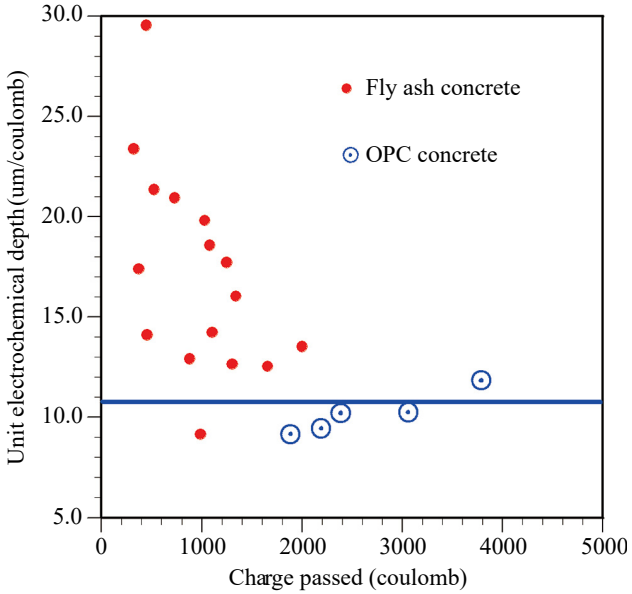

Fig. 5. Unit electrochemical depth and charge passed.

$$d = 1.50 \times 10^{-3} Q. \quad (5)$$

The correlation coefficient R^2 was 0.75. The chloride penetration depth and the charge passed were poorly correlated for fly ash concrete.

We calculated the unit electrochemical depth in the non-steady migration state (d/Q: chloride penetration depth divided by charge passed). The unit electrochemical depth and the charge passed are compared in Fig. 5, which illustrates that the OPC specimen has almost the same unit electrochemical depth for each value of charge passed, but the fly ash concrete specimen yields a chaotic result. It is a limitative that using the charge passed to estimate the chloride penetration depth just for fly ash concrete. A comparison between OPC and fly ash concrete in terms of charge passed and chloride penetration depth is shown in Fig. 6. The charges passed during RCPT indicate that OPC has a higher permeability than fly ash concrete at the same w/b ratio, but the penetration depths after RCPT illustrate that the chloride penetration depths of both concrete specimens are approximately equal: 0.6–0.9 cm. RCPT significantly overestimated the durability of fly ash concrete.

The chloride profiles of F0-30 and F20-65 concretes are shown in Fig. 7. The charge passed through the F0-30 mix (OPC concrete) was approximately 1.1 times higher than that passed through the F20-65 mix (fly ash concrete). Based on

Table 4. Rating of chloride permeability of concrete.

Chloride permeability	Based on	
	Charge (Coulomb)	Chloride penetration depth (cm)
High	>4000	> 4.66
Moderate	2000 - 4000	1.82 – 4.66
Low	1000 -2000	0.40 – 1.82
Very low	<1000	<0.40

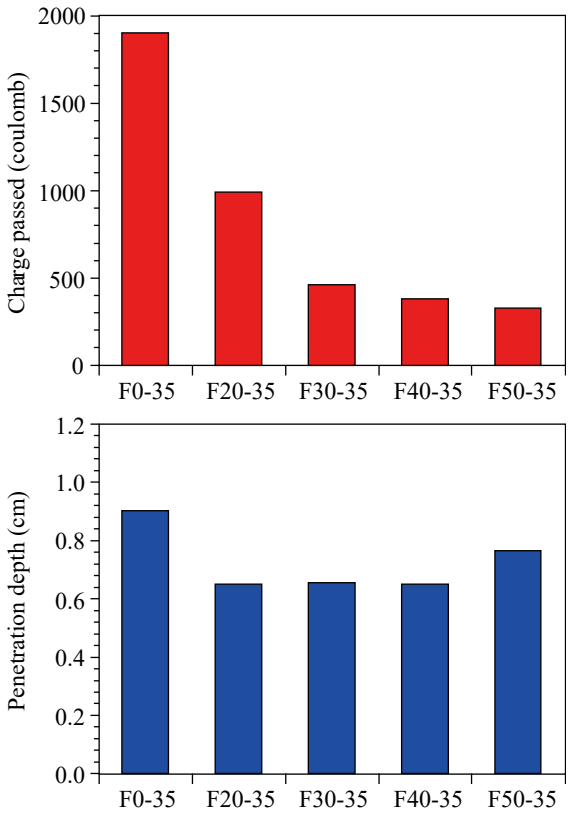

Fig. 6. The comparison between charge passed and penetration depth

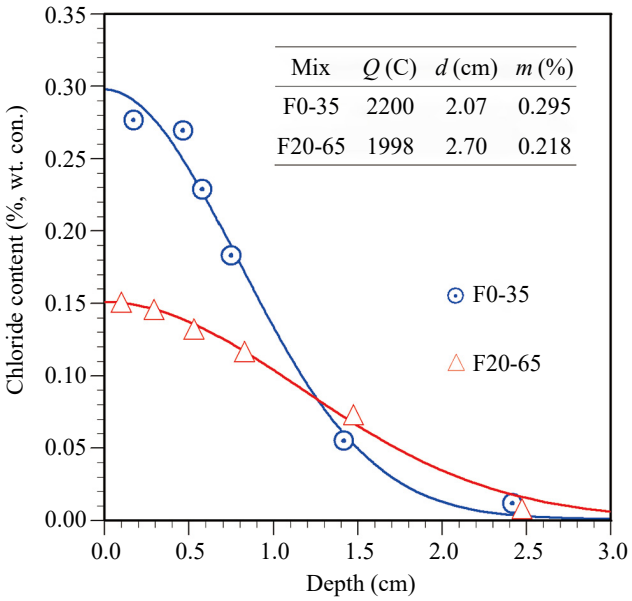

Fig. 7. The chloride profiles for F0-30 and F20-65.

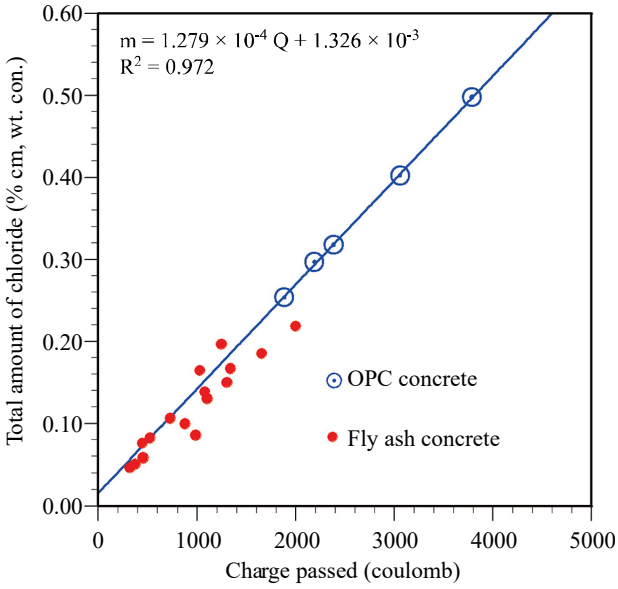

Fig. 8. The relationship between the charge passed and the total amount of chloride.

the charge passed, the permeability of F20-65 is lower than that of F0-30. However, the chloride penetration depth of F20-65 is nearly 1.3 times higher than that of F0-30, as shown in Fig. 6. Engineers are concerned with the advance of the critical chloride front toward steel and not with near-surface chloride concentrations. The values of charge passed through the specimens suggest that the chloride permeability of F20-65 is poorer than that of F0-30, whereas the chloride penetration depth of F20-65 is higher than that of F0-30. Therefore, improving RCPT is crucial for overcoming this problem.

2.3. Total amount of chloride and charge passed

In this study, we determined the total amount of chloride migration into the specimen obtained in the RCPT. The total amount of chloride in a specimen (Fig. 3) was determined by integrating the chloride profile curve as follows:

$$m = \int C dx, \tag{6}$$

where

m: total amount of chloride (%, wt. specimen).

Eq. (6) was used to determine the total amount of chloride m obtained from the chloride profiles of all mixes, as listed in Table 3. The total amount of chloride increased as the w/b ratio increased for all the series. For a given w/b ratio, the total amount of chloride in the concrete with fly ash was lower than that in the Portland cement concrete (F0).

Fig. 8 illustrates the relationship between the charge passed and the total amount of chloride, both obtained using RCPT for all mixes except F0-55 to F0-65. The data shown in Fig. 7 were subjected to linear regression analysis, and an empirical relationship between the charge passed and the total amount of chloride was statistically derived using

$$m = 1.279 \times 10^{-4} Q + 1.326 \times 10^{-3}. \tag{7}$$

Based on linear regression analysis, a linear relationship was found to exist between the total amount of chloride (m) and the charge passed (Q). The correlation coefficient was 0.972. According to Faraday's laws of electrolysis, the total amount of ions is directly proportional to the total charge passed during an electrochemical reaction. Therefore, regardless of the charge passed through OPC or fly ash concrete, the total amount of chloride (m) can be determined using Eq. (7). The values of charge passed (Table 2) can be used to compute the total amounts of chloride (m_Q) for all mixes (Table 5).

3. Determining chloride profile from charge passed and surface chloride content

To determine the chloride profile of a concrete specimen, many samples should be collected and ground for analysis. An alternative, less time-consuming method has been formulated to determine the chloride profile. The total amount of chloride in a specimen can be computed using the chloride profiles obtained using Eq. (6) and (2) and the following expressions:

$$m = \int C_s \exp(-ax^2) dx, \tag{8}$$

and

$$m = \frac{C_s}{2}\sqrt{\frac{\pi}{a}}. \tag{9}$$

Table 5 Main results of the predicted chloride profile

Mix	m_Q (%)	d_1 (cm)	C_1 (%)	C_{s1} (%)	a_p	d_p (cm)
F0-30	0.244	0.18	0.289	0.300	1.190	1.69
F0-35	0.283	0.18	0.276	0.283	0.786	2.06
F0-40	0.308	0.18	0.259	0.264	0.579	2.38
F0-45	0.394	0.18	0.269	0.272	0.375	2.97
F0-50	0.487	0.10	0.228	0.229	0.173	4.25
F0-55	0.550	0.10	0.136	0.136	-	-
F0-60	0.631	0.11	0.144	0.144	-	-
F0-65	0.706	0.11	0.132	0.132	-	-
F20-35	0.127	0.10	0.179	0.182	1.617	1.34
F20-45	0.168	0.10	0.170	0.172	0.821	1.86
F20-55	0.213	0.10	0.168	0.169	0.493	2.39
F20-65	0.257	0.10	0.151	0.151	0.271	3.16
F30-35	0.060	0.11	0.159	0.171	6.426	0.66
F30-45	0.113	0.11	0.160	0.163	1.625	1.31
F30-55	0.142	0.11	0.158	0.160	0.997	1.67
F30-65	0.172	0.11	0.140	0.141	0.527	2.24
F40-35	0.049	0.11	0.135	0.147	7.075	0.62
F40-45	0.068	0.11	0.123	0.127	2.697	0.97
F40-55	0.094	0.11	0.120	0.122	1.318	1.38
F40-65	0.139	0.11	0.120	0.121	0.596	2.04
F50-35	0.043	0.11	0.105	0.112	5.367	0.67
F50-45	0.059	0.11	0.091	0.093	1.970	1.06
F50-55	0.133	0.11	0.144	0.146	0.953	1.68
F50-65	0.160	0.11	0.164	0.166	0.842	1.83

The experimental constant a can be calculated as

$$a = \frac{\pi C_s^2}{4m^2}. \tag{10}$$

By substituting the value of a into Eq. (2), the chloride profile can be expressed as

$$C = C_s \exp\left(\frac{-\pi C_s^2}{4m^2} x^2\right). \tag{11}$$

Eq. (11) shows that the chloride profile can be obtained by measuring the total amount of chloride (m) and the surface chloride content (C_s).

We ground the specimens to depths of 1–3 mm from the surface after RCPT. The depths of the first slice (d_1) and the corresponding chloride contents (C_1) for all mixes were obtained from the nearest surface slice of the specimen, as summarized in Table 5. By substituting d_1, C_1, and the total amount of chloride obtained from the charge passed (m_Q) into Eq. (11), the surface chloride content (C_{s1}) was obtained through trial and error (Table 5). The total amount of chloride in a specimen (m_Q) was determined by using the total charge passed (Q) and Eq. (7), and the surface chloride content (C_{s1}) values listed in Table 5 were used in conjunction with Eq. (11) to obtain the chloride profiles of the concrete specimens. Table 5 lists the predicted experimental constant (a_p) and the chloride penetration depths (d_p) obtained from the chloride profiles.

Figures 9, 10 and 11 illustrate the predicted chloride penetration profile curves (dashed lines) and the chloride penetration profiles obtained by curve fitting the experimental data (solid line) of the F0-30, F0-35, and F20-65 mixes, respectively. The predicted chloride profile curves agree well with the chloride penetration profiles obtained by curve fitting the experimental data. Although the area under the predicted curve is slightly larger than that under the experimental data curve in Fig. 11, the difference between the predicted and experimental chloride penetration depths is smaller than 5 mm. The predicted chloride profiles in Figs. 9, 10 and 11, predicted chloride penetration profile curves obtained based on charge measurements, and the chloride content of the first slice confirm that the trial and error method can be used to evaluate the chloride profile of concrete rapidly.

The charge passed during RCPT and the chloride penetration depths obtained from the profiles of all specimens, except F0-60 and F0-65, are shown in Fig. 12. According to the Coulomb specifications listed in Table 4, the concrete containing fly ash exhibited very low chloride permeability;

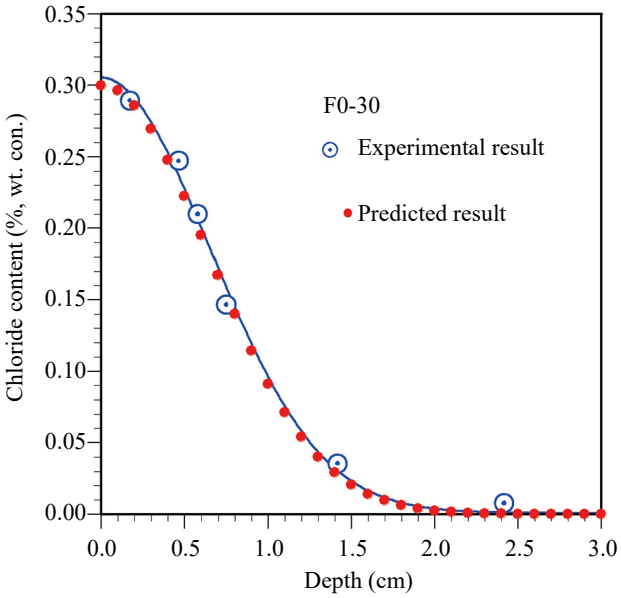

Fig. 9. The predicted curve of chloride penetration profile (dash line) and the chloride penetration profile of mix F0-30.

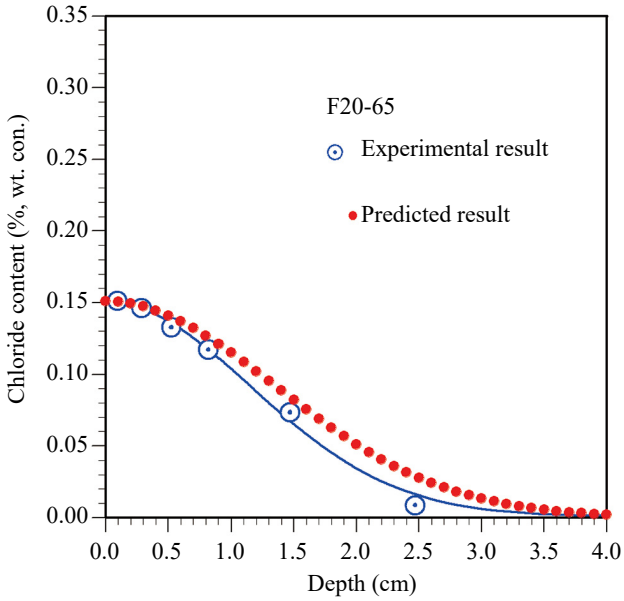

Fig. 11. The predicted curve of chloride penetration profile (dash line) and the chloride penetration profile of mix F20-65.

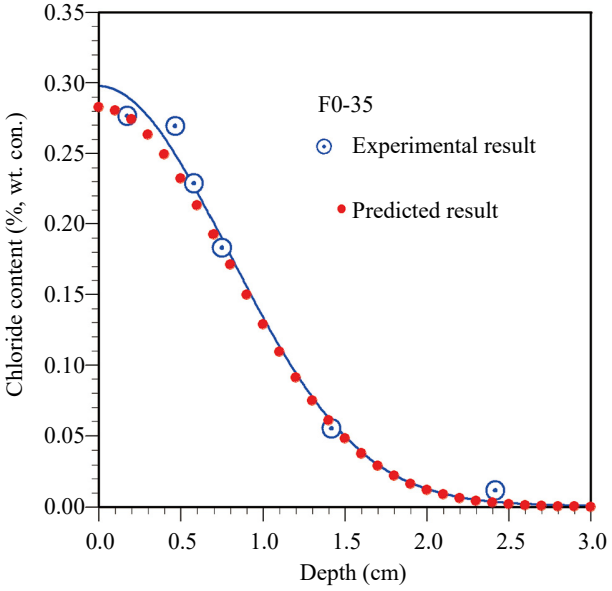

Fig. 10. The predicted curve of chloride penetration profile (dash line) and the chloride penetration profile of mix F0-35.

however, according to the chloride penetration depth specifications, the concrete containing fly ash exhibited low chloride permeability. A comparison of the charge passed and the chloride penetration depths for F0-35 and F20-65 (Fig. 7) indicates that the chloride penetration depth is an accurate criterion for assessing the chloride permeability of fly ash concrete.

4. Using penetration depth to assess chloride permeability of concrete

Concrete with fly ash can exhibit a reduced charge passed value during RCPT but its chloride penetration depth shows that it does not have low permeability. To improve RCPT for testing concrete containing supplementary cementing materials, we made the following modifications to the standard procedure:

(1) The procedure followed for RCPT was the same as that described in ASTM C1202.
(2) The value of the charge passed during RCPT was used to calculate the total amount of chloride m by using Eq. (7).
(3) After completion of RCPT, the surface chloride content C_s was determined according to the nearest surface slice measuring approximately 3 mm in thickness.
(4) The thickness of the specimen and the m and C_s values obtained in steps (2) and (3) were substituted into Eq. (11) to determine the chloride profile.
(5) The chloride penetration depth was determined using the chloride profile to assess the chloride permeability of concrete by using the data listed in Table 4.

The modified RCPT method based on the chloride penetration depth was used to assess the chloride permeability of concrete, and the penetration depth was obtained from the chloride profile. The only additional step in the modified RCPT procedure involves measuring the surface chloride content after the completion of RCPT.

IV. CONCLUSIONS

The chloride profiles were determined after the completion of RCPT. Based on the results obtained herein, the following conclusions can be drawn.

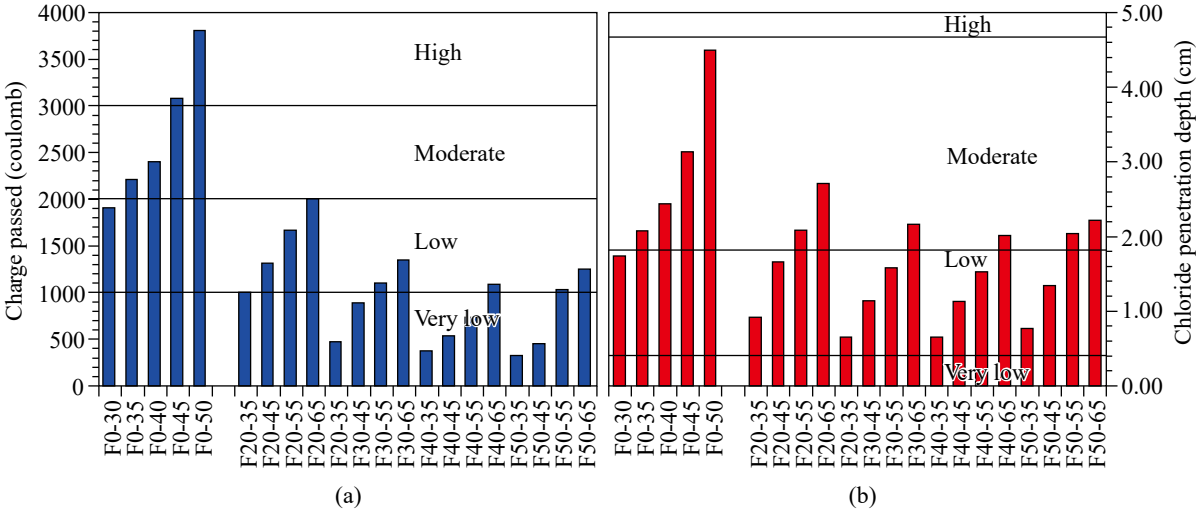

Fig. 12. The results of: (a) charge passed, and (b) the chloride penetration depths.

1. A linear relationship exists between the charge passed during RCPT and the chloride penetration depth determined using the chloride profile at the end of RCPT for OPC concrete. For OPC concrete, the chloride penetration depth can be determined by measuring the charge passed through the concrete.
2. OPC concrete had almost the same unit electrochemical depth for the mixes of OPC concrete, but the fly ash concrete presented chaotic results. For the same value of charge passed during RCPT, fly ash concrete exhibited higher a chloride penetration depth than that of OPC concrete. Thus, it is a limitative that using the charge passed to estimate the chloride penetration depth just fly ash concrete.
3. The chloride profile of a concrete can be obtained by measuring the total amount of chloride and the surface chloride content. The total amount of chloride can be determined by measuring the charge passed, and the surface chloride content can be measured after the completion of RCPT.
4. The chloride penetration depth, which was obtained from the chloride profile after the completion of RCPT, can be used to assess the chloride permeability of concrete. This method can overcome the drawbacks of using the charge passed during RCPT to rank the chloride permeability of concrete when mineral additives are used in concrete.

ACKNOWLEDGMENTS

The financial support of Ministry of Science and Technology, ROC, under the grants MOST 108-2221-E-019-008-MY2 is gratefully appreciated.

REFERENCES

Aldea, C. M., F. Young, K. Wang and S. P. Shah (2000). Effects of curing conditions on properties of concrete using slag replacement. Cement and Concrete Research 30, 465-472.

Bagheri, A. R., H. Zanganeh and M. M. Moalemi (2012). Mechanical and durability properties of ternary concretes containing silica fume and low reactivity blast furnace slag. Cement and Concrete Composite 34, 663-670.

Bernal, S. A., R. M. d. Gutierrez and J. L. Provis (2012). Engineering and durability properties of concretes based on alkali-activated granulated blast furnace slag/metakaolin blends. Construction and Building Materials 33, 99-108.

Feldman, R., Jr. L. R. Prudencio and G. Chan (1999). Rapid chloride permeability test on blended cement and other concrete: correlation between charge, initial current and conductivity. Construction and Building Materials 13, 149-154.

Julio-Betancourt, G. A. and R. D. Hooton (2004). Study of the joule effect on rapid chloride permeability values and evaluation of related electrical properties of concrete. Cement and Concrete Research 34, 1007-1015.

Lim, C. C., N. Gowripalan and V. Sirivivatnanon (2000). Microcracking and chloride permeability of concrete under uniaxial compression. Cement and Concrete Composite 22, 353-360.

McGrath, P. F. and R. D. Hooton (1999). Re-evaluation of the AASHTO T259 90-day salt ponding test. Cement and Concrete Research 29, 1239-1248.

McCarter, W. J., G. Starrs and T. M. Chrisp (2000). Electrical conductivity, diffusion, and permeability of Portland cement-based mortars. Cement and Concrete Research 30, 1395-1400.

Morozov, Y., A. S. Castela, A.P. S. Dias and M. F. Montemor (2013). Chloride-induced corrosion behavior of reinforcing steel in spent fluid cracking catalyst modified mortars. Cement and Concrete Research 47, 1-7.

Park, S. S., S. J. Kwon and S. H. Jung (2012). Analysis technique for chloride penetration in cracked concrete using equivalent diffusion and permeation. Construction and Building Materials 29, 183-192.

Pfeifer, D. W., D. B. McDonald and P. D. Krauss (1994). The rapid chloride ermeability test and its correlation to the 90-day chloride ponding test. PCI Journal 39, 38-47.

Ramezanianpour, A. A. and H. B. Jovein (2012). Influence of metakaolin as supplementary cementing material on strength and durability of concretes. Construction and Building Materials 30, 470-479.

Ravikumar, D. and N. Neithalath (2013). Electrically induced chloride ion transport in alkali activated slag concretes and the influence of microstructure. Cement and Concrete Research 47, 31-42.

Shi, C. (2004). Effect of mixing proportions of concrete on its electrical conductivity and the rapid chloride permeability test (ASTM C1202 or

ASSHTO T277) results. Cement and Concrete Research 34, 537-545.

Wee, T. H., A. K. Suryavanshi and S. S.Tin (1999). Influence of aggregate fraction in the mix on the reliability of the rapid chloride permeability test. Cement and Concrete Composite 21, 59-72.

Yang, C. C., L. C. Wang and T. L. Weng (2004). Using charge passed and total chloride content to assess the effect of penetrating silane sealer on the transport properties of concrete. Materials Chemistry and Physics 85, 238-244.

Yang, C. C. and J. K. Su (2002). Approximate migration coefficient of interfacial transition zone and the effect of aggregate content on the migration coefficient of mortar. Cement and Concrete Research 32, 1559-1565.

Yoon, S., S. Oh, J. Ha and P. M. Monteiro (2012). The effects of surface treatments on rapid chloride permeability tests. Materials Chemistry and Physics 135, 699-708.